Available online at www.sciencedirect.com
ScienceDirect
ELSEVIER
Palaeogeography, Palaeoclimatology, Palaeoecology 242 (2006) 188–200
PALAEO
www.elsevier.com/locate/palaeo

Pliocene Arctic temperature constraints from the growth rings and isotopic composition of fossil larch

A.P. Ballantyne [a,*,1], N. Rybczynski [b,1], P.A. Baker [a], C.R. Harington [b], D. White [c]

[a] Nicholas School of the Environment and Earth Sciences Duke University, Durham NC 27707, United States
[b] Canadian Museum of Nature, Ottawa, Ontario, K1P 6P4, Canada
[c] Department of Energy, Mines, and, Resources, Whitehorse, Yukon, Y1A 6E7, Canada

Received 19 September 2005; received in revised form 24 May 2006; accepted 31 May 2006

Abstract

Instrumental records reveal that the current rate of Arctic warming greatly exceeds mean global warming. However, Arctic temperatures during the Pliocene were considerably warmer than present, making it an excellent time period for investigating potential consequences of current warming trends. Here we focus on an early Pliocene (4 to 5 Ma) peat deposit from Ellesmere Island, characterized by a remarkable fossil assemblage representative of a modern boreal forest. Among the fossils are well-preserved samples of an extinct larch (*Larix groenlandii*), which were exploited as an archive of paleoclimatic information. We reconstruct Pliocene terrestrial temperatures in the high Arctic using a novel approach that combines measurements of ring-width and oxygen isotopes. This technique was calibrated by analyzing modern analog larch growing at the northern extent of their range and accounting for biotic fractionation of oxygen isotopes using a global database of modern trees. Based on this approach, we estimated mean annual temperature in the Arctic during the Pliocene to be -5.5 ± 1.9 °C, indicating that Arctic temperatures were 14.2 °C warmer than today. This more precise multi-proxy estimate is slightly warmer than previous estimates derived from empirical evidence and general circulation models. Our results also demonstrate that the biotic fractionation of oxygen isotopes in cellulose is non-linear and dependent upon regional factors affecting aridity, such as latitude and elevation. Therefore the simultaneous measurement of oxygen isotopes and morphological characteristics in paleovegetation can be useful in constraining climatic variables of Earth's past.

Keywords: Pliocene; Temperature; Isotopes; Multi-proxy; Paleoclimate; Fossil wood

1. Introduction

Climate researchers have identified the Arctic as a region of heightened concern because the rate of temperature increase in the Arctic greatly exceeds that of the global mean. Current estimates of Arctic warming are an astounding 1 °C increase in 20 years (Arctic Climate Impact Assessment, 2004). However, studies investigating global patterns of past climate variability have concluded that Arctic temperatures tend to be more variable than low-latitude temperatures (CLIMAP, 1981; Dowsett et al., 1996). Marine isotopic records indicate that for most of the past 65 million years temperatures were warmer than today, with global deep-

* Corresponding author.
E-mail address: apb14@duke.edu (A.P. Ballantyne).
[1] These authors contributed equally to this work.

0031-0182/$ - see front matter © 2006 Elsevier B.V. All rights reserved.
doi:10.1016/j.palaeo.2006.05.016

sea temperatures peaking around 12 °C during the early Eocene climatic optimum around 50–52 million years ago (Zachos et al., 2001). Subsequent to this climatic optimum, temperatures fluctuated, but generally followed a cooling trend until the onset of the Pleistocene, 1.8 million years ago (Zachos et al., 2001). Fossil evidence from high latitudes indicates that during the early Pliocene (5 Ma) the planet had cooled sufficiently to produce Arctic temperature regimes similar to modern (White et al., 1997; Elias and Matthews, 2002). This cool period was followed by a sudden Arctic warming of approximately 10 °C around 4 million years ago (Elias and Matthews, 2002) and later by the mid-Pliocene thermal optimum (Dowsett, 2004).

Estimates of past temperature also provide critical evidence for developing and validating global climate models (Sloan et al., 1996; Dowsett et al., 1999; Elias and Matthews, 2002). Paleotemperature estimates derived from polar regions are of particular interest because of the heightened climate sensitivity in these regions (Dowsett et al., 1996, 1999). The Pliocene (1.8–5.0 Ma) has received particular attention because it represents a recent period in Earth's history when global temperatures were significantly warmer than today, but without the frequent and high amplitude glacial–interglacial cycles characteristic of the Quaternary (Crowley, 1996). This period of warmth is associated with a reduction of Arctic terrestrial ice cover and an increase in sea surface temperatures of the Northern Atlantic and Pacific (Haywood et al., 2001). Although observations of fossilized marine bivalves from a single deposit in Iceland suggests an overall cooling throughout the Pliocene, these observations also document several discrete warm events (Buchardt and Símonarson, 2003). Most importantly, this Pliocene warm period appears to have arisen during a time in which Earth's orbital parameters were similar to today (White et al., 1997; Elias and Matthews, 2002; Dowsett et al., 2004), and thus may provide a realistic reference for future warming scenarios due to increased greenhouse gases (Crowley, 1996). This study contributes to the characterization of Arctic Pliocene terrestrial climate with the ultimate goal of better understanding the effect of climate warming on the evolution and distribution of Arctic biota.

Temperature is the most important determinant of the distribution, abundance, and phenotype of organisms today (Turner, 2004; Whitfield, 2004); consequently, changes in environmental temperature can be inferred from the fossil record. Previous research has demonstrated the utility of pollen (e.g. Dowsett, 2004; e.g. White et al., 1997), insects (e.g. Elias and Matthews, 2002), vertebrates (e.g. Markwick, 1998), and leaf margin shape (Wolfe and Upchurch, 1989; Spicer et al., 2002; Fricke and Wing, 2004) in reconstructing terrestrial temperatures of the past. However, investigating biotic response to changing climate requires an independent temperature proxy. Thus isotopic analysis of fossil material has emerged as a practical and powerful tool (Koch, 1998; Fricke and Wing, 2004). With the availability of independent paleotemperature estimates it has become possible to test hypotheses concerning the biotic response to temperature fluctuations. Results so far suggest that climate, specifically temperature, has played an important role in the evolution of terrestrial communities and lineages (Beard and Dawson, 1999; Smith and Betancourt, 2003; Callaghan et al., 2004).

There are very few sites in the Arctic with well-preserved plant, vertebrate and invertebrate remains; in this regard, the Beaver Pond locality (78° 33′ N; 82° 25′ W), located on Ellesmere Island is exceptional (Fig. 1). Preserved within the same stratigraphic unit at the locality are many plant remains, including pollen and wood, diatoms and other silicious microfossils, freshwater mollusk, insect, fish, bird and mammal remains. The plant macrofossils and insect remains are indicative of a Pliocene boreal forest margin community, differing somewhat from Canada's present boreal forest. The mammalian assemblage includes a relative of the black bear relative (*Ursus abstrusus*), beaver (*Dipoides* spp.), rabbit (*Hypolagus*), deerlet (new genus similar to *Blastomeryx*), hipparionine horse (c.f. *Plesiohipparion*), and a meline badger (*Arctomeles*) among others. There is some evidence of North American affinity, but most taxa (e.g. bear, deer, horse, and badger) are more closely related to taxa in Eurasia (Tedford and Harington, 2003). Although most of the fossils represent extinct taxa, their nearest living relatives are found thousands of kilometers to the south, implying considerably warmer conditions on Ellesmere Island during the Pliocene.

Earlier studies have suggested that the Beaver Pond locality was 3.5 million years old (Harington, 2001; Elias and Matthews, 2002), but subsequent estimates based on the mammalian fauna indicate that the deposit is between 4 and 5 million years old (Tedford and Harington, 2003). This new estimate is important because it places the Beaver Pond locality in a period that is not well represented by other terrestrial Arctic studies (White et al., 1997; Elias and Matthews, 2002).

Because the locality has such a diverse assemblage of well-preserved fossils, we are able to compare several different proxies of past temperature from a single location. Based on changes in the assemblage of fossil

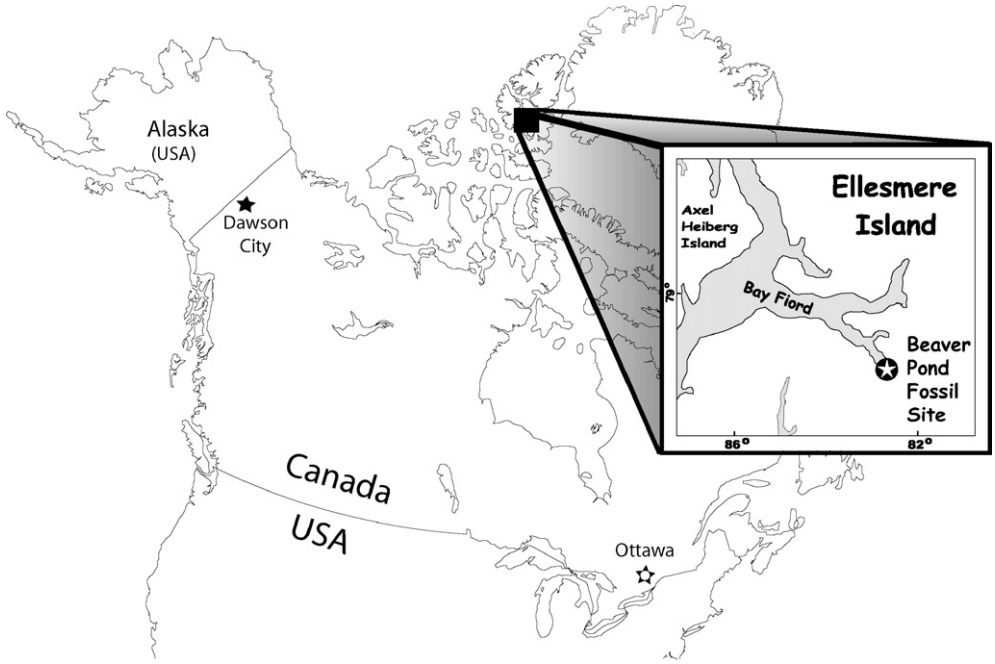

Fig. 1. Map of northern North America showing location of Beaver Pond fossil locality, and locations of modern wood samples: Dawson City, Yukon and Ottawa, Ontario.

beetles from the same Beaver Pond locality, Elias and Matthews (2002) estimated Pliocene temperatures 10–15 °C greater than present on Ellesmere Island. Although shifts in the ranges of organisms provide a very intuitive measure of climate variability, biologically derived temperature proxies tend to be less precise than geochemical proxies (Ballantyne et al., 2005). The objective of this study is to reconstruct the surface air temperature of Ellesmere Island during the Early Pliocene (4–5 Ma) by measuring the oxygen isotopic composition and ring widths of an extinct fossil larch (*Larix c.f. groenlandii*). Here we employ a novel technique by devising a temperature transfer function based on *both* the ring-width *and* oxygen isotopic composition of modern analog larch trees (*Larix* spp.) growing near the northern extent of their range in Canada. This technique relies on independent biotic (ring-width) and geochemical (oxygen isotopes) proxies from the same sample and thus is less subject to bias from any one proxy.

1.1. Oxygen isotopes in cellulose and temperature estimates at high latitudes

Libby and Pandolfi (1974) first suggested that the isotopic composition of cellulose in modern trees could function as a "paleothermometer". Pioneering work was also done by Gray and Thompson (1976), who investigated the isotopic composition of modern trees growing near the northernmost extent of their range and derived a significant empirical relationship between mean annual temperature (MAT) and the oxygen isotopic ratio of cellulose. More recently, the isotopic variability in fossil samples of *Metaseqouia* has been measured to infer paleoclimatic conditions of the Arctic during the Eocene (Jahren and Sternberg, 2002). Based on their analysis, Jahren and Sternberg (2002) argue that temperature alone could not account for the extremely depleted oxygen isotope values in the cellulose of their *Metaseqouia* samples, but that additional depletion may have arisen from distillation of distant source water. However, it is difficult to infer multiple environmental variables (e.g. temperature and source water) from a single empirical parameter (oxygen isotopes). Subsequent analyses of δD in these same *Metaseqouia* samples have revealed that the Eocene Arctic atmosphere contained approximately twice the amount of atmospheric water as today (Jahren and Sternberg, 2003). Here we employ a similar approach to constrain paleotemperature estimates from the Arctic, but we exploit measures of oxygen isotopes in conjunction with ring widths from a well-preserved Pliocene wood specimen.

Researchers interested in plant physiology have developed mechanistic models describing the physical and biological processes affecting the oxygen isotopic

composition of cellulose (Roden et al., 1999). The oxygen isotopic ratio of cellulose is referred to as $\delta^{18}O_{cx}$, where $\delta^{18}O$ is the conventional notation for the ratio of oxygen isotopes (O^{18}/O^{16}) in the sample (R) with respect to a standard (R_{st}), such that $\delta=(R/R_{st}-1)\times 1000$. For isotopic ratios of oxygen, all results are reported as $\delta^{18}O‰$ with respect to the Vienna Standard Mean Ocean Water or V-SMOW ($R_{st}=2.0052\times 10^{-3}$). The isotopic ratio of oxygen in cellulose ($\delta^{18}O_{cx}$) results from an admixture of meteoric source water absorbed by the roots ($\delta^{18}O_{sw}$) and leaf water ($\delta^{18}O_{lw}$) that has undergone evaporative enrichment (Roden et al., 1999):

$$\delta^{18}O_{cx} = f_o \cdot (\delta^{18}O_{sw} + \varepsilon_o) + (1 - f_o) \cdot (\delta^{18}O_{lw} + \varepsilon_o) \quad (1)$$

where f_o is the proportion of the carbon-bound oxygen that exchanges with source water. This fraction f_o has been empirically constrained to 0.42 at varying levels of humidity. The $\delta^{18}O$ of cellulose is enriched ($\varepsilon_o=27‰$) with respect to both source water and leaf water, due to the carbonyl–water interaction during biosynthesis (Sternberg and DeNiro, 1983).

Therefore we can introduce a new term describing the net fractionation of oxygen isotopes ($\Delta^{18}O$) that captures these constant values and also accounts for the enrichment of leaf water:

$$\delta^{18}O_{sw} = \delta^{18}O_{cx} - \Delta^{18}O \quad (2)$$

Although the enrichment of leaf water is a complex physical process primarily controlled by temperature-dependent kinetic fractionation (Majoube, 1971), we can approximate $\Delta^{18}O$ by measuring the $\delta^{18}O_{cx}$ of modern trees growing in locations where the seasonal values of $\delta^{18}O_{sw}$ in precipitation have been measured. There is an empirical relationship ($n=60$, $R^2=0.17$) between oxygen isotopes in precipitation ($\delta^{18}O_{sw}$) and temperature during the growth season at Eureka, Ellesmere Island (IAEA/WMO, 2004). Therefore, by measuring the $\delta^{18}O_{cx}$ of modern analog larch samples growing in regions where the $\delta^{18}O_{sw}$ of precipitation is known, we may calibrate the "paleothermometer", enabling us to independently estimate temperatures of the environment in which the fossil Ellesmere larch was growing. One caveat to this method is that the modern relationship between $\delta^{18}O_{sw}$ and temperature is highly variable according to region and this relationship may have been different during the Pliocene than today (Fricke and Wing, 2004).

An alternative approach to estimating the paleotemperature involves the application of two independent predictor variables to better constrain our approximation of surface air temperature (SAT). Our two temperature-dependent variables are the width of annual growth rings (R) and the oxygen isotopic composition of cellulose within the annual rings. The growth of modern larch in Siberia is known to be highly correlated with growth season temperature (Antonova and Stasova, 1997), and the fractionation of oxygen isotopes at high latitudes is also correlated with temperature, albeit with some regional variability. By measuring both of these variables in modern larch trees growing at the northern limits of their range, we can derive a multivariate model of the form:

$$SAT = \beta_0 + \beta_1 \cdot R + \beta_2 \cdot \delta^{18}O + \varepsilon \quad (3)$$

where β_o is the y-intercept, β_1 is the coefficient for ring width and corresponds to the slope of the relationship between SAT and annual tree growth, and β_2 is the coefficient for $\delta^{18}O$ in source water ($\delta^{18}O_{sw}$) or cellulose ($\delta^{18}O_{cx}$) and corresponds to the slope of the relationship between SAT and oxygen isotopes at high latitude. Lastly, ε represents the standard error term. Thus, the model can be optimized by using either $\delta^{18}O$ measured in the cellulose or the precipitation. If the model is optimized using the modern relationship between $\delta^{18}O_{sw}$ and precipitation, then we must account for biotic fractionation ($\Delta^{18}O$) when estimating paleotemperatures during the Pliocene, resulting in added uncertainty. Model coefficients are derived empirically rather than theoretically and thus may change dependent upon the particular taxa analyzed or geographical location. Although these coefficients are empirically fitted to the data, *a priori* physical knowledge suggests that a positive relationship should be observed between $\delta^{18}O$ and temperature, as well as between ring width and temperature. This multivariate approach is not exclusive to inferring climate variability from isotopes and growth in trees, but may be applied to other paleoclimatic inquiries where data from multiple proxies are available.

Although modern larch only grow for a few months during the boreal summer, they utilize both precipitation occurring during the growth season and snow melt as water sources (Sugimoto et al., 2002). Therefore, we used mean annual values of $\delta^{18}O_{sw}$ as a time-integrated signal of source water for input to our model. Both proxies of paleotemperature (i.e. R and $\delta^{18}O$) have their shortcomings; however, by combining the two proxies in a single model we ensure a more robust estimate of paleotemperature, even if the assumptions of any one proxy are violated.

Finally, we estimate the difference in surface air temperature (Δ SAT °C) on Ellesmere during the

Pliocene, as the difference between estimated surface air temperature during the Pliocene and the modern mean annual temperature (MAT) of Eureka on Ellesmere Island (Δ SAT °C = SAT − MAT), where MAT = −19.7 °C at Eureka today, based on the mean from 1947 to 1991 (Global Historical Climate Network,cdiac.esd.ornl.gov/ghcn/ghcn.html).

2. Methods

2.1. Sample collection

Samples of fossil wood that were removed from the permafrost were almost perfectly preserved and showed no signs of diagenesis. Fossil wood specimens collected from the Beaver Pond locality were identified as the extinct larch species *Larix groenlandii* (Matthews and Ovenden, 1990), which is most closely related to extant taxa growing in North America. Modern analog samples of *L. laracina* were acquired from two North American sites — Dawson, Yukon (64° N, 139° W) where MAT = −4.3 °C and Ottawa (45° N, 75° W) where MAT = 6.0 °C. The Dawson site is close to the northern extent of the range for modern larch, whereas Ottawa is close to the southern extent of the range.

2.2. Sample preparation and ring measurement

Thin cross-sections were cut laterally through samples, yielding disks that were then mounted on an aluminum plate. The working surface of each disk was sanded with progressively finer sandpaper and polished to highlight the contrast between growth rings (Fig. 2). Annual rings were identified and measured using an advancing measurement table. At least two radial transects of ring width measurements were taken per sample. Annual rings were then sub-sampled from both modern and fossil wood using a micromill (Merchantek, CA) equipped with a 0.5 mm diameter carbide bit (Dremel©). Concentric sample trajectories were mapped out using imaging software and then superimposed on the actual sample for drilling (Merchantek EO, CA). Samples were carefully monitored during drilling to avoid burning of wood that may result in isotopic fractionation. The pulverized samples were collected with a dental probe and placed in microcentrifuge tubes for cellulose extraction. Pulverized modern samples were virtually identical to pulverized fossil samples, suggesting that the fossil samples were well preserved with no evidence of diagenesis (Fig. 2).

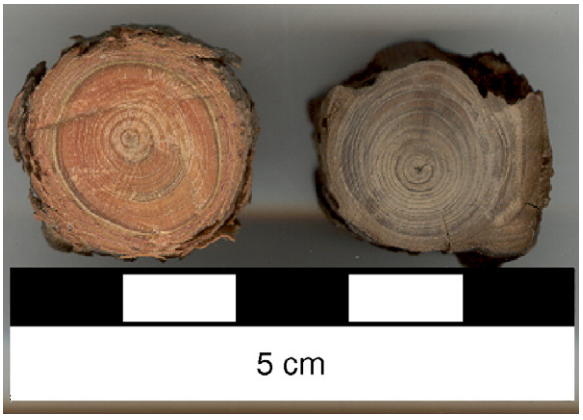

Fig. 2. Scanned image of modern larch sample from Ottawa (left) juxtaposed with fossil larch sample from Ellesmere Island (right). Note similar diameters and the presence of annual growth rings in both samples.

Although the extraction of cellulose was previously a laborious task (Leavitt and Danzer, 1992), recent advances have greatly expedited extraction resulting in greater throughput while using less harmful solvents. In some instances isotopic analysis has been performed on whole wood samples; however, this technique may result in the loss of isotopic variability (Borella et al., 1999). Because of the ease of extraction and the elimination of compounds that may confound our isotopic signal, we extracted the cellulose from samples prior to isotopic analysis. Cellulose was extracted according to the protocol of Brendel et al. (2000), which was revised for small sample amounts. According to this technique, samples were acidified and heated to remove superfluous tannins and resins followed by a series of rinsing and centrifuging steps. Samples were then dried in an oven at 60 °C for 24 h and stored in an anoxic dessicator for 24 h. Dry samples were individually weighed and packaged in silver capsules for analysis of $\delta^{18}O_{cx}$.

We measured oxygen isotopes using continuous flow mass spectrometry. Although continuous flow mass spectrometry sacrifices some precision, measurement error is 0.2‰, which is reasonable given the intra-annual variability of $\delta^{18}O$ in precipitation (IAEA/WMO, 2004) typical of modern Canada (12‰) and Ellesmere Island (16‰). Homogenized samples (~200 μg) were thermally converted in the absence of oxygen (Finnigan MAT TC/EA) and then conveyed to the mass spectrometer (Finnigan MAT Delta plus XL) in a helium stream for the separation of ^{18}O and ^{16}O. All isotopic values are reported as $\delta^{18}O$‰ with respect to V-SMOW.

The multivariate model predicting SAT was fit using a generalized linear model. To account for ontogenetic effects, all ring-width time series were detrended by

Table 1
Comparison of temperature transfer functions and their estimates of Pliocene temperatures in the Arctic

Modern temperature transfer functions	# of modern trees sampled	Coefficients $\delta^{18}O$				Ring width				Pliocene temperature	Estimates
		β_o	SE±	β_1	SE±	β_2	SE±	R^2	AIC	MAT	ΔT
Cellulose $\delta^{18}O$[a] Gray and Thompson (1976)	1	−20.5	0.2	1.3	0.1			0.88		−0.7	19.0
Cellulose $\delta^{18}O$[a] Burk and Stuiver (1981)	5	−22.97		0.41	0.2			0.94		−8.3	11.4
Cellulose $\delta^{18}O$[a] Jahren and Sternberg (2002)	12	−21.0		0.4				0.71		−3.5	16.2
Cellulose $\delta^{18}O$[b]	2	−53.2	5.6	2.29***	0.2			0.85	89.9	−8.3	11.4
Ring-width[b]	2	−6.6	2.1			0.013**	0.003	0.49	112.7	−0.7	19.0
Cellulose $\delta^{18}O$+ ring-width[b]	2	−56.5	5.3	2.43***	0.2	0.005*	0.002	0.88	86.7	−8.8	10.9
Precip $\delta^{18}O$[bc]	2	16.9	1.0	0.93****	0.06			0.96	31.4	−4.9	14.8
Precip $\delta^{18}O$+ ring-width[bc]	2	17.5	1.8	0.98****	0.1	−2.71	6.3	0.97	33.2	−5.5	14.2

Previously published temperature transfer functions based on the $\delta^{18}O$ of cellulose ($\delta^{18}O_{cx}$) compared with temperature transfer functions derived from annual ring width and $\delta^{18}O$ of cellulose and precipitation in the present study. Where β_o represents the *y*-intercept of the transfer function and the coefficients β_1 and β_2 represent the slope parameters for $\delta^{18}O$ and ring width, respectively.
[a]Transfer functions originally derived to predict $\delta^{18}O_{cx}$, thus they are of the form $MAT=(\delta^{18}O_{cx}+\beta_o)/\beta_1$.
[b]Transfer functions from the present study, such that $MAT=\beta_o+\beta_1\ \delta^{18}O+\beta_2$ ring width.
[c]Based on the relationship in Fig. 4, mean precipitation $\delta^{18}O$ was −23.5‰.
Significant transfer function coefficients are indicated by: **p*-value<0.05; ***p*-value<0.01; ****p*-value<0.001; and *p*-value<0.0001.

fitting a negative log model and then using residual values as predictor variables in the multivariate model. Independently, both $\delta^{18}O_{cx}$ ($R^2=0.85$, $P<0.001$) and ring width ($R^2=0.49$, $P<0.01$) in modern larch were significant predictors of temperature (Table 1), but the strongest individual predictor of modern temperatures was $\delta^{18}O_{sw}$ in precipitation ($R^2=0.92$, $P<0.0001$). Ultimately, the optimal multivariate model for the prediction of modern temperature was derived from the $\delta^{18}O_{sw}$ and ring width measurements ($R^2=0.93$, $P<0.0001$) from the modern analog trees (Table 1). Therefore the most robust model for the prediction of temperatures during the Pliocene is derived from $\delta^{18}O_{sw}$ and ring width, requiring us to account for the biological fractionation (i.e. $\Delta^{18}O$) of source water in our fossil larch. All statistical analyses were performed using the open source base R package (www.r-project.org).

3. Results

The mean value of $\delta^{18}O_{cx}$ in the fossil larch was 19.6‰ with little variability between years ($\sigma=0.45$‰), which is markedly lower than cellulose values obtained from other extant taxa from the literature (Table 2) and within the range of values reported for fossil *Metasequoia* growing in the Arctic during the Eocene (16‰ $<\delta^{18}O_{cx}<$21‰; see Jahren and Sternberg, 2003). The mean $\delta^{18}O_{cx}$ value from our fossil larch was most similar to the $\delta^{18}O_{cx}$ value for our modern analog larch (21.5‰) growing at the northern extent of its range in the Yukon. Generally trees growing at high latitude or high elevation tended to have greater discrimination factors ($\Delta^{18}O$) against the isotopic composition of source water (Table 2). The discrimination of oxygen isotopes was strongest in trees growing in the Altiplano of Bolivia ($\Delta^{18}O=45.0$‰), the Yukon ($\Delta^{18}O=43.8$‰) and Bern, Switzerland ($\Delta^{18}O=40.3$‰), which were all well above the mean value for reported tree species (Table 2). To better approximate the distribution of biotic fractionation in these tree species, values were re-sampled using a bootstrap yielding a normal distribution with a global mean value of $\Delta^{18}O=36.9$‰ (Supplemental Fig. 1).

Ring-widths from both the modern and fossil larch showed a gradual decline with age (Fig. 3), which characterizes the growth of most temperate trees growing at high latitudes. The absolute growth and temporal trend in growth of the fossil larch was most similar to that of the modern tree growing in the Yukon, as evidenced by the ring width measurements. The mean

Table 2
Comparison between reported values and present estimates of discrimination ($\Delta^{18}O$) between oxygen isotope values in source water ($\delta^{18}O_{sw}$) and cellulose ($\delta^{18}O_{cx}$) providing a global distribution from several taxa

Taxa	Location	$\delta^{18}O_{cx}$	$\delta^{18}O_{sw}$	$\Delta^{18}O$	Study
Larix groenlandia	Ellesmere Island, CAN (80.0° N, 85.0° W)	19.6	30.5[a]	?	Fossil; present study
Larix laricina	Ottawa, CAN (45.0° N, 75.0° W)	25.8	−11.4	37.2	Modern; present study
Larix laricina	Dawson City, CAN (61.0° N, 135.0° W)	21.5	−22.3	43.8	Modern; present study
Tamarix jordanis	Israel (31.0° N, 35.0° W)	32.6	−4.4[b]	37.0	(Lipp et al., 1996)
Pinus radiata	Balmoral, NZ (42.5° S, 172.4° E)	30.5	−8.1[c]	38.6	(Barbour et al., 2002)
	Matangi, NZ (37.5° S, 175.2° E)	30.0	−5.5[c]	35.5	
	Kawerau, NZ (38.1° S, 176.4° E)	29.0	−4.5[c]	33.5	
Pinus torreyana	La Jolla, USA (32.7° N, 117.2° W)	30.8	−4.4	35.2	(Burk and Stuiver, 1981)
Picea sitchensis	Arcata, USA (41.0° N, 124.1° W)	27.6	−6.9	34.5	
Picea sitchensis	Thorne Bay, USA (55.7° N, 135.5° W)	23.9	−11.3	35.2	
Pseudotsuga menziesii	Tyee, USA (48.1° N, 120.2° W)	26.9	−7.7	34.6	
Picea glauca	Fairbanks, USA (64.8° N, 148.1°W)	21.8	−16.6	38.4	
Santolina chanaecyprisus	Israel (31.0° N, 35.0° W)			19.4	(Wang et al., 1998)[d]
Myrtus communis				12.7	
Crataegus momogyna				22.8	
Calocedrus decurrens var 1				45.0	
Calocedrus decurrens var 2				60.2	
Styrax officinalis				49.6	
Pinus cabiniana				45.0	
Picea abies	Bern, Switzerland (47.0° N 15.0° E)	29.0	−8.0	40.3	(Anderson et al., 1998)
Salix arctica	Axel Heiberg Island (79.0° N, 89.0°W)		41.4		(Jahren and Sternberg, 2003)
Salix arctica				42.7	
Metasequoia glyptostroboides	Kyoto, Japan (34.5° N, 134.5°E)			33.7	
Metasequoia glyptostroboides	Tanashi, Japan (35.7° N, 139.5° E)			35.2	
Metasequoia glyptostroboides				36.1	
Cedrella spp.	Puerto Maldonado, Peru (15.0° S, 70° W)	25.2	−4.0	29.5	(Ballantyne et al., 2005)
Polylepis tarapacana	Altiplano, Bolivia (17.0° S, 75.0° W)	29.0	−16.0	45.0	(Ballantyne et al., 2005)
	Mean	28.1	−9.3	37.1	

[a]Annual mean $\delta^{18}O_s$ of modern precipitation at Eureka site on Ellesmere Island (IAEA/WMO, 2004).
[b]$\delta^{18}O_{sw}$ measured in stem water.
[c]$\delta^{18}O_{sw}$ extrapolated by authors from nearby sites based on temperature, precipitation and elevation.
[d]$\delta^{18}O_{cx}$ measured in exotic trees growing in a botanical garden at the same latitude.

annual ring width for the fossil larch was 473±130 μm (mean±σ) and statistically indistinguishable (P=0.543) from the modern Yukon larch (407±216 μm yr^{-1}), whereas the mean ring width for the modern Ottawa larch was significantly higher 790±455 μm yr^{-1} (P=0.005). The statistically higher growth rates in conjunction with the higher $\delta^{18}O_{cx}$ values in the modern Ottawa larch are indicative of warmer temperatures, resulting in enhanced growth.

The main assumption of our study is that trees are faithful recorders of the isotopic composition of source water used in the synthesis of cellulose. Therefore there should be a predictable relationship between the isotopic composition of cellulose and that of precipitation. If we plot $\delta^{18}O$ of precipitation as a function of $\delta^{18}O$ in cellulose for a range of taxa distributed around the world (Fig. 4; hereafter referred to as GIP-C model), we see that there is, in fact, a strong statistical relationship between these variables (R^2=0.84). However, it is not linear, but rather follows an exponential curve. Trees with relatively enriched $\delta^{18}O$ cellulose values, with respect to $\delta^{18}O$ of precipitation, tend to be from high latitude or high elevation locations characterized by a more arid climate, thereby resulting in greater evaporative enrichment of leaf water (i.e. increased $\Delta^{18}O$). In contrast, trees with relatively depleted values of cellulose $\delta^{18}O$ are found in more humid environments, typically at low latitude or elevation. Anomalous values that deviate from this pattern provide information about the local environment in which these trees were growing. For instance, the $\delta^{18}O$ of cellulose from *Polylepis* spp. growing in the tropics at 4500 m was far more enriched than we would

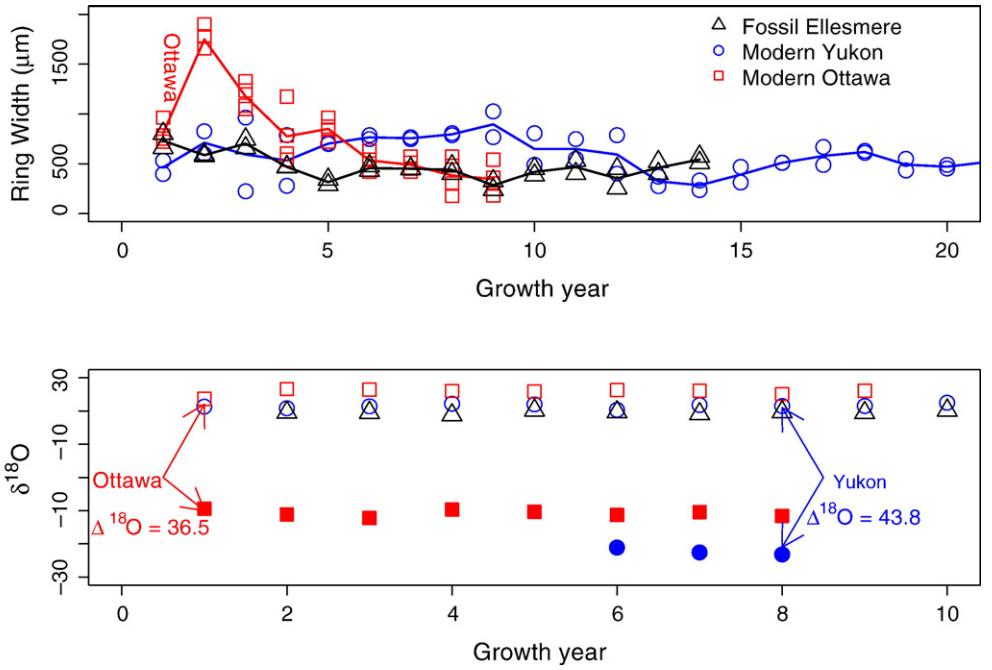

Fig. 3. Annual ring width measurements (μm) for the initial 20 years of growth for both fossil and modern larch samples (top panel). Solid lines represent mean values for each specimen. Oxygen isotope values for modern precipitation (filled symbols) compared with cellulose values (unfilled symbols) for overlapping growth years in samples (bottom panel). Annotated is the isotopic enrichment of cellulose above precipitation for larch growing at the modern sites.

have predicted based upon the $\delta^{18}O$ of precipitation. This enrichment is due to the arid environment in which this genus grows (mean annual precipitation 0.316 m). Conversely, based on the cellulose $\delta^{18}O$ of a *Cedrella* spp. growing in the Peruvian Amazon we would predict a moderately depleted $\delta^{18}O$ of precipitation. Instead, we observe a precipitation $\delta^{18}O$ that is highly enriched because this tree was growing on the eastern slope of the Andes, which is extremely wet (mean annual precipitation >2.0 m).

Because there has been no appreciable change in the latitude or elevation of Ellesmere Island since the Pliocene, we can use this relationship to predict the $\delta^{18}O$ of Pliocene precipitation on Ellesmere. Based on the isotopic values of cellulose measured in our fossil larch, we estimate the mean $\delta^{18}O_{sw}$ in precipitation to be −23.5‰, resulting in a relatively high biotic fractionation ($\Delta^{18}O=43.0$‰) indicative of arid conditions on Ellesmere Island during the Pliocene (Supplemental Fig. 1). This inferred value of −23.5‰ for the isotopic composition of Pliocene precipitation on Ellesmere Island is appreciably enriched compared to modern annual precipitation at Eureka Bay ($\delta^{18}O_{sw}=-30.5$‰).

Although the empirical relationship between oxygen isotopes in cellulose and precipitation is statistically robust, the coefficients affecting the GIP-C model may have differed during the Pliocene and thus we should entertain scenarios that may have affected this relationship. The first factor that undoubtedly affected the global distribution of oxygen isotopes in precipitation is changes in global ice volume. If we consider the Pliocene as a heightened inter-glacial period, in which very little ^{16}O was captured in continental ice, we would expect much more ^{16}O circulating through the global hydrologic cycle, resulting in a reduced global mean $\delta^{18}O_{sw}$ This global ice volume change would cause a negative shift in the intercept of the GIP-C model (upper grey line in Fig. 4), thereby decreasing our estimate of oxygen isotope concentration in precipitation during the Pliocene. If we assume a 1‰ decrease in global mean $\delta^{18}O_{sw}$ during the Pliocene, then this results in only a negligible change in our isotopic estimate of local Ellesmere precipitation during the Pliocene ($\delta^{18}O_{sw}=-23.5$‰). Conversely, the warmer climatic conditions that prevailed during the Pliocene resulted in increased atmospheric water vapor, thereby reducing evaporation rates and causing a negative shift in the $\delta^{18}O_{cx}$ values of our GIP-C model (lower grey line in Fig. 4). If we assume a 1‰ decrease in $\delta^{18}O_{cx}$ values due to increased humidity during the Pliocene, this results in a considerable increase in our estimate of the isotopic composition of precipitation ($\delta^{18}O_{sw}=-26.8$‰). Therefore changes

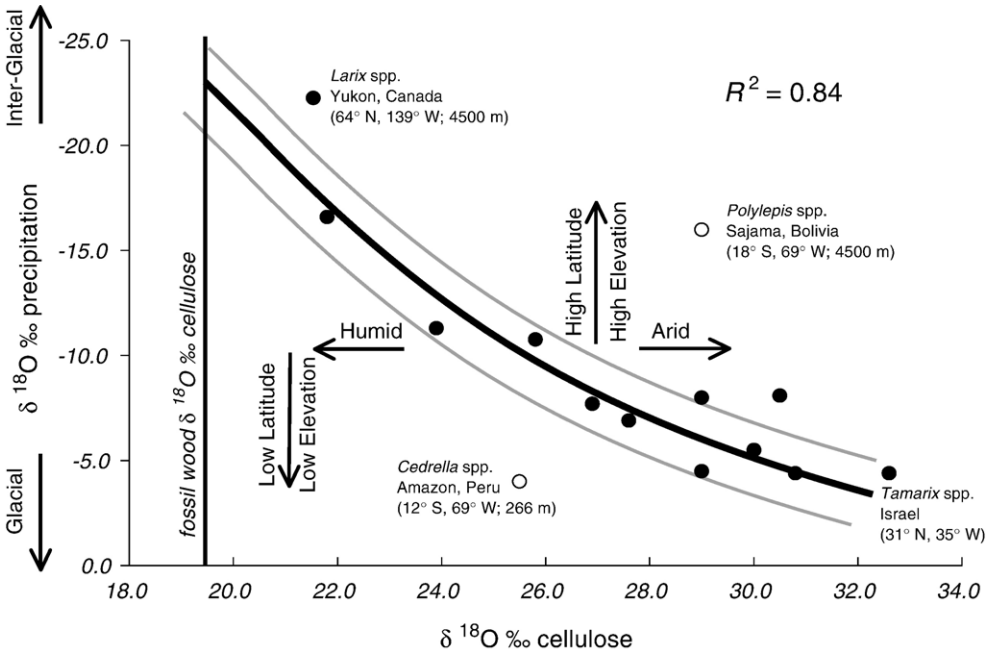

Fig. 4. Global relationship between the $\delta^{18}O$ of cellulose and the $\delta^{18}O$ of precipitation. The GIP-C model (solid black curve) of the form $abs(\delta^{18}O‰ \text{ precipitation}) = 312.75 \times e^{(-0.13 \times \delta\ 18\ O‰\ \text{cellulose})}$ has been fitted to observations from Table 1 (filled circles) with an R^2 of 0.84. Anomalous values from high elevation locations in the Andes and the lowland Amazon (unfilled circles) were excluded from model formulation. The mean oxygen isotopic value of fossil wood from Ellesmere Island ($\delta^{18}O = 19.6‰$) is plotted as a solid vertical line. The grey curves represent potential past scenarios when the global curve may have been shifted due to increased atmospheric moisture (shifted left) and/or heightened interglacial conditions (shifted up).

in the amount of atmospheric vapor are probably more important than changes in global ice volume in determining the oxygen isotopic composition in palaeovegetation.

Because there is very little analytical error associated with the measurement of $\delta^{18}O_{cx}$ (~0.2‰) and the standard errors of our transfer function are very minimal (Table 2), most of the error that arises in our estimate of $\delta^{18}O_{sw}$, and ultimately temperature, is due to uncertainty in the GIP-C model. Therefore we can use the GIP-C model to predict $\delta^{18}O_{sw}$ using the two Pliocene scenarios (i.e. heightened interglacial and increased

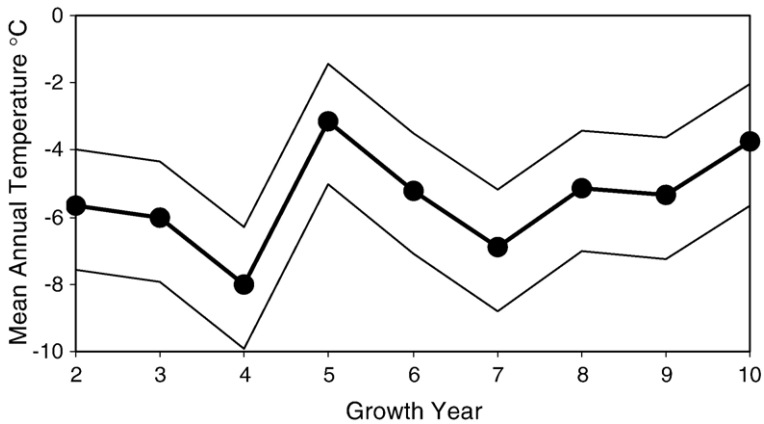

Fig. 5. Mean annual temperature estimates for the Pliocene on Ellesmere Island based on cellulose $\delta^{18}O$ and ring width measurements from fossil larch. Mean estimates (filled circles) based on the modern GIP-C model (see Fig. 4) are bound by estimates based on the heightened interglacial model (lower limit) and the humid model (upper limit).

humidity) as error terms to bound our temperature estimate. This approach yields a Pliocene MAT for Ellesmere Island of −5.5 °C, with an upper limit of −3.8 °C and a lower limit of −7.4 °C (Fig. 5 and Table 2). This estimate corresponds with a 14.2 °C increase in Arctic temperatures during the Pliocene compared to today. We consider this to be the most constrained estimate based upon ring-width and isotopic data presented herein and isotopic values reported in the literature.

4. Discussion

Our estimate of SAT = −5.5 ± 1.9 °C on Ellesmere Island, corresponding to a 14.2 °C Arctic warming during the Pliocene, is within the range of previously derived empirical estimates of mean annual temperature but is slightly higher than temperature estimates during the growth season. Previous estimates of warming from this site derived from assemblages of fossil beetles yielded a range in Pliocene temperatures from 10 to 15 °C warmer than present (Elias and Matthews, 2002), with greater warming occurring in the winter (15 °C) than the summer (10 °C). Because our independently derived estimate of temperature lies near the warmer limit of this range, we may infer that a winter temperature signal is being captured by the $\delta^{18}O_{cx}$. In fact, this is true of modern larch growing at high latitude, which often utilize seasonal melt water from snow that accumulated during winter months (Sugimoto et al., 2002). All of our temperature estimates, regardless of which transfer function was used, yielded estimates that exceeded 10 °C of Arctic warming during the Pliocene (Table 1), indicating that the fossil larch sampled in this study was probably integrating an annual temperature signal. Of the independent temperature transfer functions, obtained from the literature and derived from this study, 3 of our 8 temperature estimates exceeded 15 °C, suggesting that Pliocene temperatures in the Arctic may have been slightly warmer than indicated by previous estimates.

Another potential explanation reconciling the slightly different temperature estimates derived from fossil beetle assemblages and isotopes in trees is the phenology of larch trees. Larch is one of the few conifers that are deciduous. According to the fossil evidence, the boreal forest that covered Ellesmere during the Pliocene was dominated by larch (Tedford and Harington, 2003). The annual flushing of leaves during the boreal summer may have reduced direct incident insolation, thereby reducing ground surface temperatures more in the summer than the winter. However much of the disparity in seasonal temperatures was probably compensated by the increased albedo of snowcover during the boreal winter. It is also noteworthy that the modern distribution of *Larix laricinia* (USGS, http://climchange.cr.usgs.gov/data/atlas/little/), which has the most northern range of any *Larix* spp. in North America, is largely restricted to regions with mean annual temperatures ranging from −5 to 5 °C (National Snow and Ice Data Center, http://nsidc.org/fgdc/maps/gtmap_can_us_browse.html). Therefore, if similar physiological constraints existed for larch during the Pliocene, then Ellesmere Island was probably close to the northern limit of their range.

Our approximation of SAT is also slightly warmer than GCM results, which suggest that the High Arctic latitudes were only ~10 °C warmer during the Pliocene than today (Sloan et al., 1996). Moreover, GCM simulations of the Pliocene revealed only slight warming during the boreal summer in the Northern Hemisphere, with most of the temperature increase occurring during winter months, resulting in reduced seasonality. The physical explanation offered for this phenomenon is that increased cloud cover over the ocean during summer months resulted in increased albedo, in turn decreasing the amount of solar radiation reaching Earth's surface. Whereas the lack of sea ice during winter months allows for oceanic heat loss thereby warming the atmosphere. In contrast, our estimates suggest much warmer SAT, certainly during the boreal summer when our fossil larch was growing, and probably throughout the year. Larch phenology can also be invoked as an explanation for the disparity in these temperature estimates as the loss of leaves during winter months can greatly increase the albedo, thereby decreasing temperatures during the boreal winter. Previous model simulations of the Pliocene (Sloan et al., 1996; Haywood et al., 2001) have prescribed evergreen forest as the boundary conditions for the high Arctic (Thompson and Fleming, 1996; Dowsett et al., 1999). Furthermore climate models that include a dynamic vegetation component often predict the expansion of evergreen needle leaf forests at high latitude (Haywood and Valdes, 2006). Although evergreen forest vegetation is probably an accurate representation of the Arctic energy balance during summer months, it may underestimate albedo during winter months. Based on similar general circulation simulations of Cretaceous climates it was concluded that low albedo deciduous forests may significantly enhance high latitude warming (Otto-Bliesner and Upchurch, 1997).

Modern transfer functions, based upon oxygen isotopic ratios in cellulose, vary widely in their

predictions of temperature (Table 1). Because published transfer functions have a range of intercepts (−20.5 to −22.97) and slopes (0.4 to 1.3) they yield vastly different temperature estimates, especially for the Pliocene (−8.3 to 0.7 °C). However, our independent estimate based on oxygen isotopes and ring widths (5.5 °C) is bracketed quite well by estimates derived from these previously published transfer functions. The spurious estimates of past temperature derived from modern isotope-temperature transfer functions have previously been mentioned (Fricke and Wing, 2004) and even Epstein et al. (1977) cautioned that, "the $\delta^{18}O$ of the cellulose does not serve as a sensitive or reliable indicator of temperature between regions or species." This is probably due in part to the non-linear relationship between cellulose $\delta^{18}O$ and that of precipitation (Fig. 4); and even this tenuous relationship fails to predict the $\delta^{18}O$ of precipitation in extremely arid or humid environments. The correspondence between temperature predictions from our multi-variate approach and that from a range of transfer functions based solely on $\delta^{18}O_{cx}$ suggest a robust relationship between oxygen isotopes in vegetation and temperature, albeit with regional variability. However, our best temperature estimates derived solely from $\delta^{18}O_{cx}$ (11.4 °C) or ring width (19.0 °C) were markedly different, suggesting that these proxies may be biased towards extreme temperature estimates. Therefore the inclusion of multiple proxies in our model allowed for more precise predictions of past temperature that were less sensitive to biases associated with any individual proxy.

Although a significant relationship was observed between our proxies and temperature and this relationship proved useful in constraining estimates of Arctic surface temperatures during the Pliocene, these predictions were based on only two modern larch samples and one fossil larch sample. Despite our small sample size of modern trees our transfer function based solely on $\delta^{18}O_{cx}$ is remarkably similar to the transfer function derived by Burk and Stuiver (1981) for a series of coastal pine trees growing along a latitudinal gradient in North America. In fact, the two transfer functions arrive at identical estimates of −8.3 °C for the Arctic during the Pliocene (Table 1), suggesting that the isotopic composition of trees growing at high latitude is an effective proxy of temperature. However, because this temperature estimate is lower than the range of temperatures bracketing the distribution of modern larch (−5 to 5 °C), predictions of past temperature may be improved by including additional climate proxies (i.e. annual ring width) in the analysis. Our predictions of Pliocene Arctic temperatures were based on measurements from a single intact piece of fossil wood, which may not be representative of the forest growing on Ellesmere at this time. However, subsequent analyses of Pliocene-aged fossil larch samples collected at a different location on Ellesmere Island show a similar range in oxygen isotope values between 18 and 20‰, indicating a fairly coherent isotopic signal in the precipitation of Ellesmere Island during the Pliocene (Csank et al., 2006). A more extensive sampling and analysis of both modern and fossil wood is currently underway for the upcoming International Polar Year (IPY 2007–2008).

We cannot preclude the possibility that our observation of highly enriched $\delta^{18}O_{cx}$ in the fossil larch collected from Ellesmere Island is at least partly due to changing origins of $\delta^{18}O_{sw}$. Changes in source water have been argued to explain the abnormally low $\delta^{18}O_{cx}$ values in Eocene-age fossil wood from a nearby site. However, due to changes in continental configurations during the Eocene, there was much less open ocean between Ellesmere Island and the Equator (Zachos et al., 2001). Therefore there was probably much less exchange of atmospheric water with ocean water as it was advected poleward during the Eocene. In contrast, during the Pliocene the continents were in a similar configuration to today, allowing for exchange between atmospheric moisture and seawater. Further, model simulations of the Pliocene show no increase in the extent of Hadley circulation or major deviations in the jet stream (Sloan et al., 1996), implying similar source regions for water in the precipitation of Ellesmere Island today. Finally, it is known that sea level was approximately 35 m. higher during the Pliocene and that this increase corresponded with a depletion of $\delta^{18}O$ of seawater between −0.2 and −0.5‰ (Buchardt and Símonarson, 2003). Such a small change in $\delta^{18}O_{sw}$ of local precipitation is negligible compared with the estimated change from Pliocene to the present (7.0‰). Therefore the most parsimonious argument is that the depleted $\delta^{18}O_{cx}$ in the fossil wood of Ellesmere Island largely reflects increased temperatures during the Pliocene.

Several lines of evidence suggest that the paleoenvironment of Ellesmere during the Pliocene was similar to that of the modern Yukon Territory of Canada. First, the mean ring widths from the fossil sample collected at Ellesmere and the modern sample from the Yukon are statistically indistinguishable. This implies that both ecosystems experienced a similar number of warm days during the growth season, despite the greatly reduced photoperiod at the latitude of Ellesmere Island. Second, the mean $\delta^{18}O_{cx}$ value for our fossil sample (19.6‰)

was most similar to the contemporary sample collected from Dawson City (21.5‰). Further, the approximated Pliocene values of oxygen isotopic composition in the precipitation at Ellesmere ($\delta^{18}O_{sw}=-23.5‰$) is close to that of the modern Yukon ($\delta^{18}O_{sw}=-22.3‰$). Moreover, the assemblage of fossils excavated from the Beaver Pond Locality is characteristic of modern taxa located at the northern margin of the current boreal forest — a biome that dominates the Yukon Territory of today. Finally, our SAT estimate for Ellesmere Island during the Pliocene (−5.5 °C) is remarkably close to that of Dawson City today (−4.3 °C). Collectively, these observations give credence to the notion that the Pliocene on Ellesmere Island may have resembled the contemporary Yukon, both in terms of climatic regime and biotic composition.

If the Beaver Pond locality is indeed early Pliocene in age (4–5 Ma), and our estimate of SAT is accurate, then this suggests greater warmth at the beginning of the Pliocene followed by a gradual cooling. Funder et al. (1985) estimated that Arctic temperatures were only 6 °C warmer during Pliocene–Pleistocene transition (2 Ma) in Northern Greenland. This would indicate an 8 °C cooling of Arctic temperatures during the Pliocene, which is consistent with the global marine temperature curve (Zachos et al., 2001), which shows a gradual cooling over this period. Alternatively, it is possible that the warm climate of the Beaver Pond locality represents a discrete peak of warmth during the early Pliocene. This observation may be corroborated by a pronounced warm event, as observed in the marine fossil record of Iceland (Buchardt and Símonarson, 2003), that occurred at approximately the same time. A similar thermal optimum has been documented in the North Pacific at approximately 3.95 million years ago (Heusser and Morley, 1996). If these events were circumpolar and coeval, then perhaps the Pliocene was punctuated by multiple warm events followed by a gradual cooling.

As global temperatures increase, especially at high latitudes, the ranges of organisms will undoubtedly be affected. By characterizing the climate and the biotic composition of Ellesmere Island during the Pliocene, we may gain a glimpse of what future warming holds for Arctic Ecosystems.

Acknowledgments

We are grateful to Jonathan Karr and the staff at the Duke Environmental Isotope Laboratory for their assistance with the isotopic analysis. We would also like to thank Pippa McNeil for collecting modern analog samples from Dawson City, Yukon Territory. We appreciate Donna Naughton's assistance with figure preparation. We also appreciate the access to the Merchantek, micromill in the laboratory of Drew Coleman, University of North Carolina, Chapel Hill. Michael Evans of the University of Arizona provided the revised cellulose extraction protocol. Fieldwork was supported by the Canadian Museum of Nature, and the Polar Continental Shelf Project (Canada). Previous versions of this manuscript benefited from comments by Harry Dowsett, Tom Crowley, Gary Dwyer, and one anonymous reviewer.

Appendix A. Supplementary data

Supplementary data associated with this article can be found, in the online version, at doi:10.1016/j.palaeo.2006.05.016.

References

Arctic Climate Impact Assessment, 2004. In: Hassol, S.J. (Ed.), Executive Summary. Cambridge University Press, UK.

Anderson, W.T., Bernasconi, S.M., McKenzie, J.A., Saurer, M., 1998. Oxygen and carbon isotopic record of climatic variability in tree ring cellulose (Picea abies): an example from central Switzerland (1913-1995). Journal of Geophysical Research 103 (D24), 31,625–31,631.

Antonova, G.F., Stasova, V.V., 1997. Effects of environmental factors on wood formation in larch (*Larix sibirica* Ldb.) stems. Trees 11, 462–468.

Ballantyne, A.P., Lavine, M., Crowley, T.J., Liu, J., Baker, P.B., 2005. Meta-analysis of tropical surface temperatures during the Last Glacial Maximum. Geophysical Research Letters 32 (L05712).

Barbour, M.M., Walcroft, A.S., Farquhar, G.D., 2002. Seasonal variation in d13C and d18O of cellulose from growthrings of Pinus radiata. Plant, Cell and Environment 25, 1483–1499.

Beard, K.C., Dawson, M.R., 1999. Intercontinental dispersal of Holarctic land mammals near the Paleocene/Eocene boundary: paleogeographic, paleoclimatic and biostratigraphic implications. Bulletin de la Société Géologique de France 170 (5), 697–706.

Borella, S., Leuenberger, M., Saurer, M., 1999. Analysis of $\delta^{18}O$ in tree rings: wood-cellulose comparison and method dependent sensitivity. Journal of Geophysical Research 104 (D15), 19267–19274.

Brendel, O., Iannetta, P.P.M., Stewart, D., 2000. A rapid and simple method to isolate pure alpha-cellulose. Phytochemical Analysis 11 (1), 7–10.

Buchardt, B., Símonarson, L.A., 2003. Isotope palaeotemperatures from the Tjörnes beds in Iceland: evidence of Pliocene cooling. Palaeogeography, Palaeoclimatology, Palaeoecology 189, 71–95.

Burk, R.L., Stuiver, M., 1981. Oxygen isotope ratios in trees reflect mean annual temperature and relative humidity. Science 211, 1417.

Callaghan, T.V., et al., 2004. Biodiversity, distributions and adaptations of Arctic species in the context of environmental change. Ambio 33 (7), 404–417.

CLIMAP, 1981. Seasonal reconstructions of the Earth's surface at the last glacial maximum. Geological Society of America Map Chart Series, MC-36.

Crowley, T.J., 1996. Pliocene climates: the nature of the problem. Marine Micropaleontology 27, 3–12.

Csank, A.Z., Patterson, W.P., Basinger, J.F. and Eglington, B.M., 2006. Tree-ring stable isotope evidence for NAO/PDO type cyclicity in the Early Pliocene, Masters Thesis University of Saskatchewan, Saskatoon.

Dowsett, H., 2004. Bracketing Mid-Pliocene Sea Surface Temperature: Maximum and Minimum Possible Warming. U.S. Geological Survey Data Series, vol. 114.

Dowsett, H., Barron, J., Poore, R., 1996. Middle Pliocene sea surface temperatures: a global reconstruction. Marine Micropaleontology 27 (1–4), 13–25.

Dowsett, H., et al., 1999. Middle Pliocene Paleoenvironmental Reconstruction: PRISM2. U.S. Geological Survey Open File Report, vol. 99-535.

Dowsett, H.J., Chandler, M.A., Dwyer, G.S., Cronin, T.M., 2004. Bracketing the warm peak phases of the middle Pliocene. American Geophysical Union, Annual Meeting.

Elias, S.A., Matthews, J.V., 2002. Arctic North American seasonal temperatures from the latest Miocene to the Early Pleistocene, based on mutual climatic range analysis of fossil beetle assemblages. Canadian Journal of Earth Sciences 39 (6), 911–920.

Epstein, S., Thompson, P., Yapp, C.J., 1977. Oxygen and hydrogen isotopic ratios in plant cellulose. Science 198, 1214.

Fricke, H.C., Wing, S.L., 2004. Oxygen isotope and paleobotanical estimates of temperature and delta(18) O-latitude gradients over North America during the early Eocene. American Journal of Science 304 (7), 612–635.

Funder, S., Abrahamsen, N., Bennike, O., Feyling-Hanssen, R.W., 1985. Forested Arctic: evidence from North Greenland. Geology 13 (8), 542–546.

Gray, J., Thompson, P., 1976. Climatic information from 18O/16O ratios of cellulose in tree rings. Nature 262, 481–482.

Harington, C.R., 2001. Life at a 3.5 million year old beaver pond in the Canadian Artic islands and the modern scene. Meridian 11–13 (Fall/Winter).

Haywood, A.M., Valdes, P.J., 2006. Vegetation cover in a warmer world simulated using a dynamic global vegetation model for the Mid-Pliocene. Palaeogeography, Palaeoclimatology, Palaeoecology 237, 412–427.

Haywood, A.M., Valdes, P.J., Sellwood, B.W., Kaplan, J.O., Dowsett, H.J., 2001. Modelling Middle Pliocene warm climates of the USA. Palaeontologia Electronica 4 (1).

Heusser, L.E., Morley, J.J., 1996. Pliocene climate of Japan and environs between 4.8 and 2.8 Ma: a joint pollen and marine faunal study. Marine Micropaleontology 27, 85–106.

IAEA/WMO, 2004. Global Network of Isotopes in Precipitation. The GNIP Database.

Jahrenf, A.H., Sternberg, L., 2002. Eocene meriodional weather patterns reflected in the oxygen isotopes of Arctic fossil wood. GSA Today 12 (1), 4–9.

Jahren, A.H., Sternberg, L., 2003. Humidity estimate for the middle Eocene Arctic rain forest. Geology 31 (5), 463–466.

Koch, P., 1998. Isotopic reconstruction of past continental environments. Annual Review of Earth and Planetary Science 26, 573–613.

Leavitt, S.W., Danzer, S.R., 1992. Methods for batch processing small wood samples to hollocellulose for stable-carbon isotope analysis. Analytical Chemistry 65, 87–89.

Libby, L.M., Pandolfi, L.J., 1974. Temperature dependence of isotope ratios in tree rings. PNAS 71 (6), 2482–2486.

Lipp, J., Trimborn, P., Edwards, T., Waisel, Y., Yakir, D., 1996. Climatic effects on the $\delta^{18}O$ $\delta^{13}C$ of cellulose in the desert tree Tamarix jordansis. Geochemica et Cosmochimica Acta 60 (17), 3305–3310.

Majoube, M., 1971. Fractionement en oxygéne-18 et en deutérium entre l□eau et sa vapeur. Journal of Chemical Physics 197, 1423–1426.

Markwick, P.J., 1998. Crocodilian diversity in space and time: the role of climate in paleoecology and its implication for understanding K/T extinctions. Paleobiology 24 (4), 470–497.

Matthews, J.V., Ovenden, L.E., 1990. Later Tertiary plant macrofossils from localities in Arctic/Subarctic North America: a review of the data. Arctic 43 (4), 364–392.

Otto-Bliesner, B.L., Upchurch, G.R., 1997. Vegetation-induced warming of high-latitude regions during the Late Cretaceous period. Nature 385, 804–807.

Roden, J.S., Ehleringer, J.R., Lin, G., 1999. A mechanistic model for interpretation of hydrogen and oxygen isotope ratios in tree-ring cellulose. Geochimica et Cosmochimica Acta 64 (1), 21–35.

Sloan, L., Crowley, T.J., Pollard, D., 1996. Modeling of middle Pliocene climate with the NCAR GENESIS general circulation model. Marine Micropaleontology 27, 51–61.

Smith, F.A., Betancourt, J.L., 2003. The effect of Holocene temperature fluctuations on the evolution and ecology of Neotoma (woodrats) in Idaho and northwestern Utah. Quaternary Research 59 (2), 160–171.

Spicer, R.A., et al., 2002. Palaeoenvironment and ecology of the middle Cretaceous Grebenka flora of northeastern Asia. Palaeogeography, Palaeoclimatology, Palaeoecology 184 (1–2), 65–105.

Sternberg, L., DeNiro, M.J., 1983. Biogeochemical implications of the isotopic equilibrium fractionation factor between the oxygen atoms of acetone and water. Geochimica et Cosmochimica Acta 47, 2271–2274.

Sugimoto, A., Yanagisawa, N., Daisuke, N., Noburu, F., Maximov, T., 2002. Importance of permafrost as a source of water for plants in east Siberian taiga. Ecological Research 17, 493–503.

Tedford, R.H., Harington, C.R., 2003. An Arctic mammal fauna from the Early Pliocene of North America. Nature 425, 388–390.

Thompson, R.G., Fleming, R.F., 1996. Middle Pliocene vegetation: reconstructions, paleoclimatic inferences, and boundary conditions for climate modeling. Marine Micropaleontology 27, 27–49.

Turner, J.R.G., 2004. Explaining the global biodiversity gradient: energy, area, history and natural selection. Basic and Applied Ecology 5 (5), 435–448.

Wang, X.-F., Yakir, D., Avishai, M., 1998. Non-climatic variations in the oxygen isotopic compositions of plants. Global Change Biology 4 (8), 835–850.

White, J.M., et al., 1997. An 18 million year record of vegetation and climate change in northwestern Canada and Alaska: tectonic and global climatic correlates. Palaeogeography, Palaeoclimatology, Palaeoecology 130 (1–4), 293–306.

Whitfield, J., 2004. Ecology's big, hot idea. Plos Biology 2 (12), 2023–2027.

Wolfe, J.A., Upchurch, G.R., 1989. North-American nonmarine climates and vegetation during the Late Cretaceous — reply. Palaeogeography, Palaeoclimatology, Palaeoecology 69 (1–2), 142–144.

Zachos, J., Pagani, M., Sloan, L., Thomas, E., Billups, K., 2001. Trends, rhythms, and aberrations in global climate 65 Ma to Present. Science 292 (5517), 686–693.